Journal of Thermal Engineering, Vol. 3, No. 6, Special Issue 6, pp. 1588-1606, December, 2017
Yildiz Technical University Press, Istanbul, Turkey

STUDY OF AXISYMMETRIC NATURE IN 3-D SWIRLING FLOW IN A CYLINDRICAL ANNULUS WITH A TOP ROTATING LID UNDER THE INFLUENCE OF AXIAL TEMPERATURE GRADIENT OR AXIAL MAGNETIC FIELD

S. C. Dash[1*], N. Singh[2]

ABSTRACT

The three dimensional swirling flow has been obtained by solving Navier Stokes equations, expressed in cylindrical coordinate system, using finite difference technique on a staggered grid. An explicit finite difference method using pressure correction technique, for the solution of Navier-Stokes has been implemented to solve three dimensional flows. Present study explores the 3-D axisymmetric nature of stratified swirling flow and vortex breakdown in a cylindrical annulus cavity with top rotating lid. The annulus is obtained by inserting a thin coaxial rod in cylindrical cavity. This rod may be stationary or rotating depending on the particular study. Three dimensional swirling flows in annuli have also been studied subjected to axial temperature gradient or under the influence of axial magnetic field. Influence of governing parameters Re, Ri and Ha on the overall heat transfer has been investigated through variation of the average Nusselt number with these parameters. Further, the present numerical results are shown to be in good agreement with the available benchmark solutions under the limiting conditions.

Keywords: *Three Dimensional, Swirling Flows, Magneto Hydrodynamics, Stratified Flow, Incompressible Fluid.*

INTRODUCTION

There has been interest to study swirling flow for last many decades. The swirling flow occurs in various flow devices: ranging from centrifuges used for particle separation and collection to vortex tubes used for cooling to furnaces and combustion chambers. Flow with swirl occurs in draft tubes of hydraulic turbines, as well as in the casing of the compressors and axial turbines. Practical application of study of swirling flow and vortex breakdown also ranges from vortex control on modern aircraft to mixing in combustion chambers and to chemical reactions. In another application strong magnetic field can be used in lithium-lead alloys cooling system of fusion reactor. This application can be realized by creating a liquid metal flow in a closed cylindrical cavity by rotating end wall under the influence a strong axial magnetic field.

Several investigators have focused on the issue of the axial symmetry or lack of it in the lid driven swirling flow-field. Experiments conducted by Escuder[1] indicate a small degree of asymmetry in the flow field but did not addressed this aspect adequately. Hourigan et al. [2] argued that the asymmetry seen in the experimental results, Escuder[1], is perhaps due to some unidentified errors remained in the observation techniques. However, more accurate flow visualization photographs, Steven et al.[3]; Fujimura et al.[4] ; Spohn et al.[5], too have revealed such asymmetric behavior in the swirling flow field.

As an outcome of these experimental observations it has been claimed that the vortex breakdown could be physically an asymmetric phenomenon and hence argued that previous 2-D axisymmetric simulations are unable to capture the 3-D asymmetric flow features. In some of the studies, Blackburn & Lopez[6]; Sotiropoulos & Ventikos[7]; Sotiropoulos et al.[8]; Gelfgat et. al.[9]; Serre & Bontoux[10], numerical simulations of the swirling flow have included a fully 3-dimensional model. The 3D simulations by Sotiropoulos & Ventikos[7], reconfirmed the observation of Spohn et al.[5]that the boundary layer separation along the sidewall is basically asymmetric and concluded that the dynamics of the vortex breakdown bubble is indeed a 3-D,asymmetric and unsteady phenomenon.

Escudier [1] observed the vortex breakdown phenomenon in swirling flows in a cylindrical container with a rotating lid utilizing a laser-induced-fluorescence technique. Escudier's experimental results are the extension of those obtained earlier by Vogel[8]and Ronnenberg [9]. One of the major contributions of his study was to observe and report that multiple vortex breakdown bubbles can exist in the closed cylindrical geometry. These recirculation vortex breakdown bubbles were observed to be axisymmetric and steady over a large range of the governing parameters i.e. aspect ratio (AR) and Reynolds Number (Re).

This paper was recommended for publication in revised form by Regional Editor Sandip Kale
[1]*(Phd,IIT kgp),Assistant professor(SG),Mechanical Engineering Department, JUET, Guna, MP,INDIA*
[2]*Professor, Aerospace Engineering Department, Indian Institute Of Technology, Kharagpur, West Bengal, India,*
Manuscript Received 18 October 2016, Accepted 6 June 2017
**E-mail address: subasiitkgp@gmail.com*

This study by Escudier[1] reinforced the view that the vortex breakdown in general is inherently axisymmetric and its departures from axial symmetry is due to instabilities which are not directly associated with the breakdown process earlier put forward by Escudier & Keller[10] . Lopez[11] carried out a detailed numerical study with an aim to develop a more detailed understanding of the physics of the flow and to clarify features that were not readily resolved from the visualizations. Similar to Lugt and Abboud [12], Lopez[11] too assumed an axisymmetric flow-model and solved the Navier Stokes equations using stream-function vorticity formulation but his solution procedure is quite different. Lopez[11] compared his numerical solutions in detail with available experimental results, particularly dye-streak photographs of the flow due to Escuder[1] and the extent of the agreement had been critically examined and is found to be very good. For axisymmetric case Bessai *et al.* [13] have numerical studied the steady laminar magneto hydrodynamic (MHD) flow driven by rotating disk at the top of a cylinder filled with liquid metal. Bessaı¨h *et al.* [14] extended this study. Gelfgat and Gelfgat [15] have undertaken experimental and numerical study of the flow in cylindrical enclosure driven by rotating Magnetic field (RMF).

Axisymmetric disc driven swirling flow under the influence of axial temperature gradient have been conducted by Lee and Hyun[16], Kim and Hyun[17], Lugt and Abboud [12], Iwatsu [18], . Also Chen[19] seems to be the first one to investigate entropy generation inside disk driven rotating convectional flow for axisymmetric case. Effects of partial heating of top rotating lid with axial temperature gradient on vortex breakdown in case of axisymmetric stratified lid driven swirling flow have been conducted by Dash and Singh [20].

Gefagat [21] has shown that a model problem of flow in a vertical cylinder with a parabolic temperature profile on the sidewall, isothermal top and bottom and rotating top resembles the destabilization of natural convection flow by a weak rotation, which recently was reported for different configurations of Czochralski model flow. Studying the mechanisms responsible for the destabilization it was observed that at large Prandtl number the destabilization is caused by a development of an unstable stratification below the cold top boundary. A slow rotation of the top leads to a steepening of axial temperature gradient and further destabilization of the unstably stratified region. Bessaı¨h *et al.* [22] studied the magneto-hydrodynamic stability of an axisymmetric rotating flow in a cylindrical enclosure filled with a liquid metal (Pr=0.015), having an aspect ratio AR=2, and under the combined influence of a vertical temperature gradient and an axial magnetic field. Stability of swirling flows with heat transfer generated by two rotating end disks (co- and counter-rotating) inside a cylindrical enclosure with AR=2, filled with a liquid metal, and subjected to a vertical temperature gradient and an axial magnetic field has been studied by Mahfoud and Bessaı¨h[23].However, three dimensional effects on vortex breakdown in swirling flow due to axial temperature gradient or axial magnetic field is rarely investigated. This motivates the present study, where the main objective is to examine the three dimensional effects on vortex breakdown in swirling flow due to axial temperature gradient or axial magnetic field. Because of staggered grid arrangement many of the singular terms are not required to be calculated at r=0 and hence do not cause any difficulty. However, the viscous term involving second derivative with respect to radial direction in Azimuthal momentum equation requires special treatment as discussed by various authors; Verzicco and Orlandi[24], Barbosa and Daube[25] and Fukagata and Kasagi[26]. These singularities in the present study have been avoided by considering the swirling flow in annulus cavity.

Present numerical solutions for a cylindrical cavity of AR=1.0 has been validated against those due to Iwatsu[18] for ranges of governing parameters; Reynolds number and Richardson number at fixed value of Prandtl Number Pr=1.0. The remaining study is restricted to the case of annuals cavity of AR=1.5 with varying values of Reynolds number, Richardson number and Hartmann Number with fixed value of Prandtl Number Pr=1.0.

MATHEMATICALLY FORMULATION

The three dimensional swirling flow is generated by rotating disk or lid at the top of the cylindrical annulus cavity, filled with viscous, stratified and electrical conducting fluid, with constant angular velocity. The top rotating lid of cylindrical cavity is kept at a higher temperature as compared to the bottom stationary wall, as shown in Figure 1 a), when subjected to axial heat transfer. A stable temperature gradient or constant magnetic field is maintained, between the top rotating lid and the bottom fixed wall, in axial direction in order to investigate the effects of heat transfer and/or magnetic field upon the swirling flow pattern and vortex breakdown.

Governing Equations

The non-dimensional conservative forms of 3-dimensional governing equations expressed in cylindrical coordinates are:

Continuity equation:

$$\frac{1}{r}\frac{\partial(ru)}{\partial r}+\frac{1}{r}\frac{\partial u_\theta}{\partial \theta}+\frac{\partial u_y}{\partial y}=0 \tag{1}$$

Momentum equation in radial direction:

$$\frac{\partial u_r}{\partial t}+\frac{1}{r}\frac{\partial(ru_ru_r)}{\partial r}+\frac{\partial(u_ru_y)}{\partial y}+\frac{1}{r}\frac{\partial(u_ru_\theta)}{\partial \theta}-\frac{u^2{}_\theta}{r}=$$
$$-\frac{\partial p}{\partial r}+\frac{1}{\mathrm{Re}}\left[\frac{\partial}{\partial r}\left(\frac{1}{r}\frac{\partial ru_r}{\partial r}\right)+\frac{\partial^2 u_r}{r^2\partial\theta^2}+\frac{2}{r^2}\frac{\partial u_\theta}{\partial\theta}+\frac{\partial^2 u_r}{\partial y^2}\right]+\frac{Ha^2}{\mathrm{Re}}Fl_r \tag{2}$$

Momentum equation in azimuthal direction:

$$\frac{\partial u_\theta}{\partial t}+\frac{1}{r}\frac{\partial(ru_ru_y)}{\partial r}+\frac{u_\theta u_r}{r}+\frac{1}{r}\frac{\partial(u_\theta u_\theta)}{\partial\theta}+\frac{\partial(u_yu_\theta)}{\partial y}=$$
$$-\frac{1}{r}\frac{\partial p}{\partial\theta}+\frac{1}{\mathrm{Re}}\left[\frac{\partial}{\partial r}\left(\frac{1}{r}\frac{\partial ru_\theta}{\partial r}\right)+\frac{1}{r^2}\frac{\partial^2 u_\theta}{\partial\theta^2}+\frac{2}{r^2}\frac{\partial u_\theta}{\partial\theta}+\frac{\partial^2 u_\theta}{\partial y^2}\right]$$
$$+\left(\frac{Ha^2}{\mathrm{Re}}Fl_\theta\right) \tag{3}$$

Momentum equation in axial direction:

(4)

$$\frac{\partial u_y}{\partial t}+\frac{1}{r}\frac{\partial(ru_ru_y)}{\partial r}+\frac{1}{r}\frac{\partial(u_yu_\theta)}{\partial\theta}+\frac{\partial(u_yu_y)}{\partial y^2}=$$
$$-\frac{\partial p}{\partial y}+\frac{1}{\mathrm{Re}}\left[\frac{1}{r}\frac{\partial}{\partial r}\left(r\frac{\partial u_y}{\partial r}\right)+\frac{1}{r^2}\frac{\partial^2 u_y}{\partial\theta^2}+\frac{\partial^2 u_y}{\partial y^2}\right]+Ri\times T$$

Energy Equation:

(5)

$$\frac{\partial T}{\partial t}+\frac{1}{r}\frac{\partial(ru_rT)}{\partial r}+\frac{1}{r}\frac{\partial(u_\theta T)}{\partial\theta}+\frac{\partial(u_yT)}{\partial y}$$
$$=\frac{1}{\mathrm{Re}\,\mathrm{Pr}}\left[\frac{1}{r}\frac{\partial}{\partial r}\left(r\frac{\partial T}{\partial r}\right)+\frac{1}{r^2}\frac{\partial^2 T}{\partial\theta^2}+\frac{\partial^2 T}{\partial y^2}\right]$$

Electric potential Equation:

$$\frac{1}{r}\frac{\partial}{\partial r}\left(r\frac{\partial\Phi}{\partial\theta}\right)+\frac{1}{r^2}\left(\frac{\partial^2\Phi}{\partial\theta^2}\right)+\frac{\partial^2\Phi}{\partial y^2}=\frac{u_\theta}{r}+\frac{\partial u_\theta}{\partial r}+\frac{1}{r}\frac{\partial u_r}{\partial\theta} \tag{6}$$

$$\text{Where}\quad Fl_r=u_r, Fl_y=0, Fl_\theta=\frac{\partial\Phi}{\partial r}-u_\theta. \tag{7}$$

Where the reference scale for length, time, velocity and pressure are R,Ω^{-1}, $R\Omega$ and $\rho R^2\Omega^2$ respectively. The temperature T is non-dimensionalized as $T=\frac{T-T_C}{T_h-T_C}$. where T_h & T_C are temperatures at known upper hotter & lower cooler disk respectively. For the top hotter disk a suitable external heat-source can be used to maintain the required temperature T_h. Whereas, for the lower cooler disk a suitable

heat-sink, that acts like passive heat exchanger, is usually used. It transfers the heat acquired by the lid from the fluid inside the cavity to the external liquid coolant and dissipate away and maintains the temperature at required level i.e. T_C. The side wall is perfectly insulated thermally.

The Electric potential [Φ^*]is non-dimensionalized $\Phi = \frac{\Phi^*}{(\Omega R^2 B)}$. The parameters which govern the fluid motion and temperature distribution and are used in the present study are defined: Reynolds number: $\mathrm{Re} = \frac{\Omega R^2}{\nu}$ where ν is the kinematic viscosity, Richardson Number Ri , Prandtl number: Pr. The magnitude of Ri Richardson number decides the type of convection during the flow process. The Hartmann number $Ha = BR\sqrt{\frac{\sigma}{\mu}}, [\sigma]$- The interaction parameter, the ratio of the electromagnetic force to inertia force, $N = \frac{Ha^2}{\mathrm{Re}}$.

Boundary Condition for Velocity, Temperature and Electro potential:

In the present investigation all walls of the cylindrical cavity are considered to be electrically insulated

On the surface of axial rod (inner cylinder):

$$r = 0.1, 0 \le y \le h, 0 \le \theta \le 2\pi, u_r = 0, u_\theta = 0, u_y = 0, \frac{\partial T}{\partial r} = 0, \frac{\partial \Phi}{\partial r} = 0 \quad \text{(a)}$$

On the outer vertical surface of cylinder:

$$r = 1, 0 \le y \le h, 0 \le \theta \le 2\pi \; u_r = 0, u_\theta = 0, u_y = 0, \frac{\partial T}{\partial r} = 0, \frac{\partial \Phi}{\partial r} = 0 \quad \text{(b)}$$

On the surface of bottom stationary wall:

$$y = 0, 0 \le r \le 1, 0 \le \theta \le 2\pi, u_r = 0, u_\theta = 0, u_y = 0, T = 0, \frac{\partial \Phi}{\partial r} = 0 \quad \textbf{(c)}$$

On the surface of top rotating lid:

$$y = 1.0, 0 \le r \le 1, 0 \le \theta \le 2\pi, u_r = 0, u_\theta = r, u_y = 0, T = 1.0, \frac{\partial \Phi}{\partial r} = 0 \quad \textbf{(d)}$$

Re-entering boundary conditions:

$$u_{ri,j,k_n} = u_{ri,j,k_0}, u_{\theta i,j,k_n} = u_{\theta i,j,k_0}, u_{yi,j,k_n} = u_{yi,j,k_0} \; p_{i,j,k_n} = p_{i,j,k_0},$$

$$\Phi_{i,j,k_n} = \Phi_{i,j,k_0}, T_{i,j,kn} = T_{i,j,k0}$$

where k_n is last cell and k_0 is the stating cell in azimuthal direction:

NUMERICAL TECHNIQUE AND SOLUTION PROCEDURE:

The finite difference scheme for the solution of Navier Stokes equations, expressed in cylindrical coordinates, for incompressible flow requires staggered grid arrangement: where the unknown velocity components (u_r, u_θ, u_y) and the scalar quantities pressure (p), temperature (T) and electric potential (Φ) associated with each cell are defined at different location of the cell as shown e.g. for i,j,k cell in Figure 1 b). In the present scheme the scalar quantity, p, T, Φ are stored at the center of the cell, whereas the velocity components of the velocity vector (u_r, u_θ, u_y) are stored at respective midpoints on the cell faces. The present 3-D computation has been performed in the physical domain itself. As the computational domain is cylindrical annulus it is

convenient to work in cylindrical coordinate system. An equally spaced structured grid is used with [Δr , $\Delta\theta$, Δy]the spacing in respective directions.

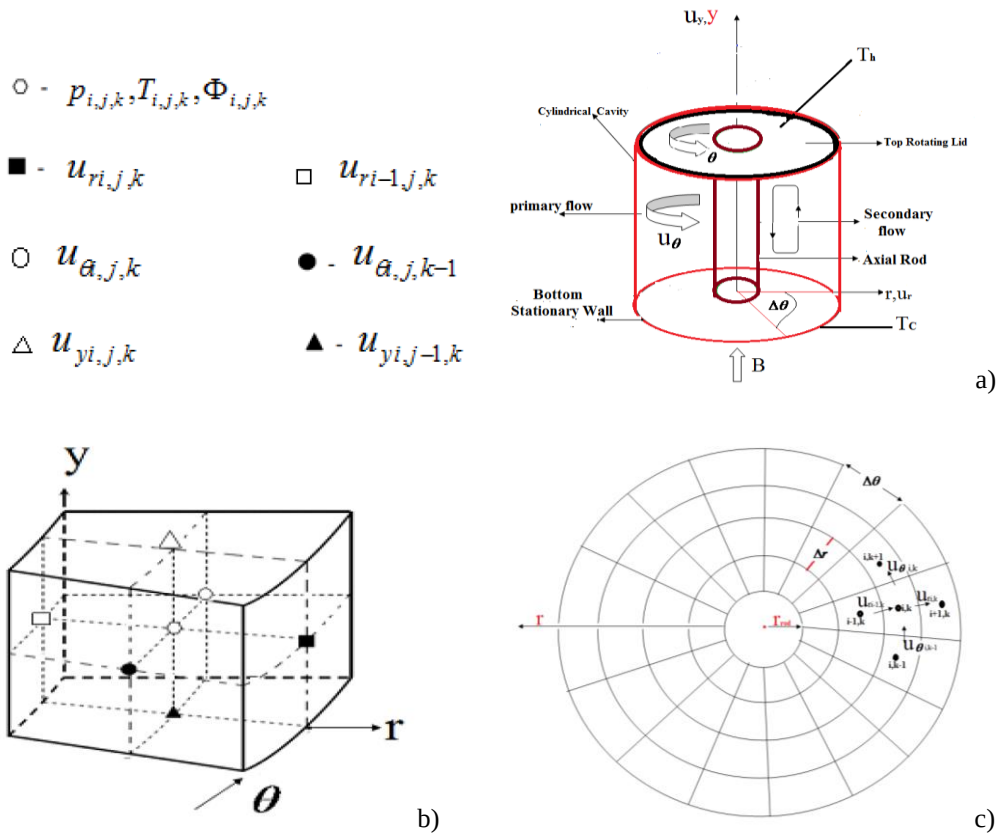

Figure 1. a) Schematic of lid-driven swirling flow in cylindrical cavity with an axial rod of aspect ratio H/R. (b) A 3-D element or cell (i, j, k) with locations of pressure, temperature, electric potential and velocity components points. (c) Top view (r $-\theta$: plane) of cylindrical cavity with staggered grid arrangement of 3-D grid.

Pressure Correction Technique:

In the present numerical scheme the convective terms in the momentum equations are discretized by central/upwind differencing where as the viscous terms are always approximated by second order central differencing. Pressure terms are also discretized using central differencing. Knowing the solution at nth time level u_r, u_θ, u_y , p, the aim is to obtain the solution at next time level. The procedure of solving radial, azimuthal and axial momentum equations is based on pressure correction technique. While advancing solution from n-th time to (n+1)th time level explicitly one get velocity field which may or may not satisfy the continuity equation. This problem is resolved by using pressure correction technique where the pressure and velocity components for each cell are corrected iteratively in such a way that for the final pressure field the velocity divergence in each cell vanishes. The iterative process is continued till the velocity divergence for each cell is less than the prescribed upper limit, for the present study it has been taken as 0.000001. Finally, the velocity boundary conditions are also corrected and one gets a divergence free converged velocity field, at (n+1)th time level, in all the cells, including the cells at the boundary. The typical features of pressure correction technique, also referred as *modified MAC* method, are available in detail in a paper by Chorin [27] and Peyter and Taylor[28] for the solution of incompressible Navier-Stoke equation in rectangular Cartesian co-ordinate system. After obtaining the corrected radial, azimuthal and axial velocity field using the above pressure correction technique, these velocity components are used to solve the energy equation and electric potential equation explicitly to get the T, Φ at (n + 1)th time level .

The solution procedure

Knowing the solution at n[th] time level $u_r, u_\theta, u_y, p, \Phi$ the aim is to obtain the solution at next time level.

The solution procedure is,

1. The momentum equations are solved following the pressure correction technique described above.
2. Subsequently: Depending on the situation either the explicit finite difference solution of energy equation 5, is obtained for temperature field T when considering effects of temperature gradient in axial direct; or the finite difference solution of the electric potential equation 6 has been obtained using relaxation technique to find electric potential when an axial magnetic field is imposed. The Lorenz force components are then calculated using Equation 7.
3. Step (1) and step (2) are repeated until convergence for the case where the steady state exits or for a required time for unsteady flow calculations.

RESULTS AND DISCUSSION:

Three dimensional flows have been simulated for AR=1.5 annular cavity for fixed value of Reynolds Number Re=1290 with the radius of inner axial rod kept as 10% of radius of lid.

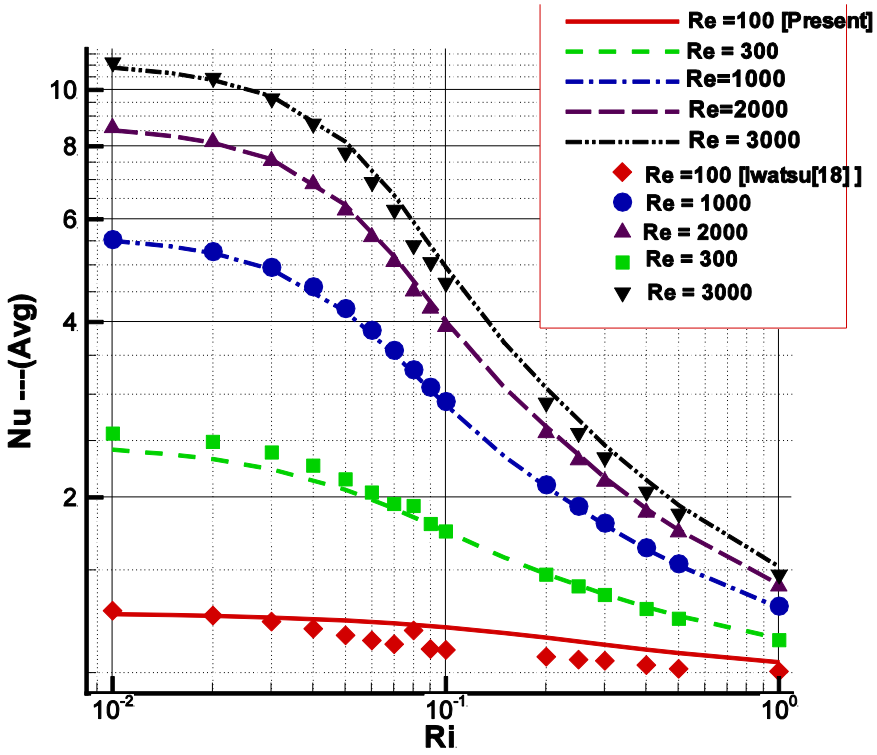

Figure 2. Comparison of average Nusselt number for AR =1.0, cavity flow with different Reynolds numbers and Richardson numbers but fixed value of Pr =1.0.

Three dimensional flows simulations are restricted to the case of annuals cavity of AR=1.5 with varying values of Reynolds number, Richardson number and Hartmann Number with fixed value of Prandtl Number Pr=1.0. Main incentive of the study is to investigate if the three dimensional laminar flow remains axisymmetric or not under the influence of axial temperature gradient or the axial magnetic field and if so how it compares with 2-D.

Validation

The present solutions for a cylindrical cavity of AR=1.0 have been validated against those due to Iwatsu [18] for ranges of governing parameters; Reynolds number $100 \le \mathrm{Re} \le 3000$ and Richardson number $0.0 \le Ri \le 1.0$ at fixed value of Prandtl Number Pr=1.0. The average Nusselt number Nu as calculated by the present code compares very well with those obtained using correlation polynomial given by Iwatsu [18], Figure 2. There are some deviations for Re=100 &3000 which may be expected as these are the end points of the range of Re for which the correlation relations had been obtained. It can be observed that the

average Nusselt number , that reflects the change of the flow structure, is a monotonically decreasing function of Ri at all Reynolds numbers.

Case I: 3-D lid driven swirling flow in a cylindrical annulus:

In the present study the behaviors of vortex breakdown in case of incompressible 3D swirling flow in a lid driven cylindrical annulus has been carried out. Figure 3 shows comparison of flow patterns in meridional plane (r-y plane) of 2-D (Axisymmetric) and 3-D calculations.

The flow pattern of 3-D calculations in various meridional planes with θ = 80; 160; 240 and 320 degrees are very similar and also compare very well with the 2-D calculations with axisymmetric assumptions. Size, shape and position of vortex break down are identical. It indicates that under the given conditions the flow remains axisymmetric. The contours of azimuthal velocity distribution in different y-constant planes, y=0.15, 0.75 and 1.35, are identical as shown in Figure 4. These contours are simply concentric circles which once again indicate the flow is axisymmetric. The region of higher azimuthal velocity, the red color region, becomes narrower and moves radial outwards as one approach toward the rotating top lid. As the flow turns out to be axisymmetric the 3-D azimuthal velocity component for any chosen θ can be considered for comparison with 2-D calculations. Comparison of 2-D and 3-D calculations of the radial profiles of azimuthal velocity in different y =0.1, 0.75, and 1.4 planes are included in Figure 5. The comparison is good that indicates the 3-D calculations are correct and the flow is essentially axisymmetric.

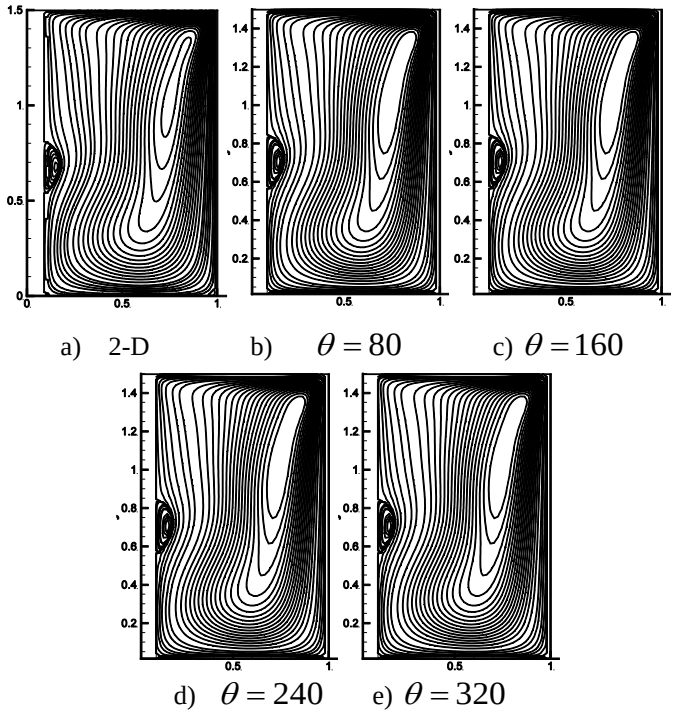

Figure 3. Contours of stream function in (r-y) meridional plane of cylindrical cavity at Re=1290, AR =1.5 at different (θ).

Case II: 3-D Lid driven swirling flow in a cylindrical annulus with application of axial Heat gradient with Pr =1.0 and Ri =0.05.

In this case, the top rotating lid temperature T_h is source isothermal and bottom stationary wall T_C is sink isothermal condition. All remaining surfaces are insulated. As a result of which an axial heat flux is imposed upon the lid driven swirling flow inside the cylindrical annulus. The axisymmetric behavior of the flow remains even under the axial heat gradient and the 3-D calculations compares very well with the present 2-D axisymmetric calculations as shown in Figure 6 to Figure 13.

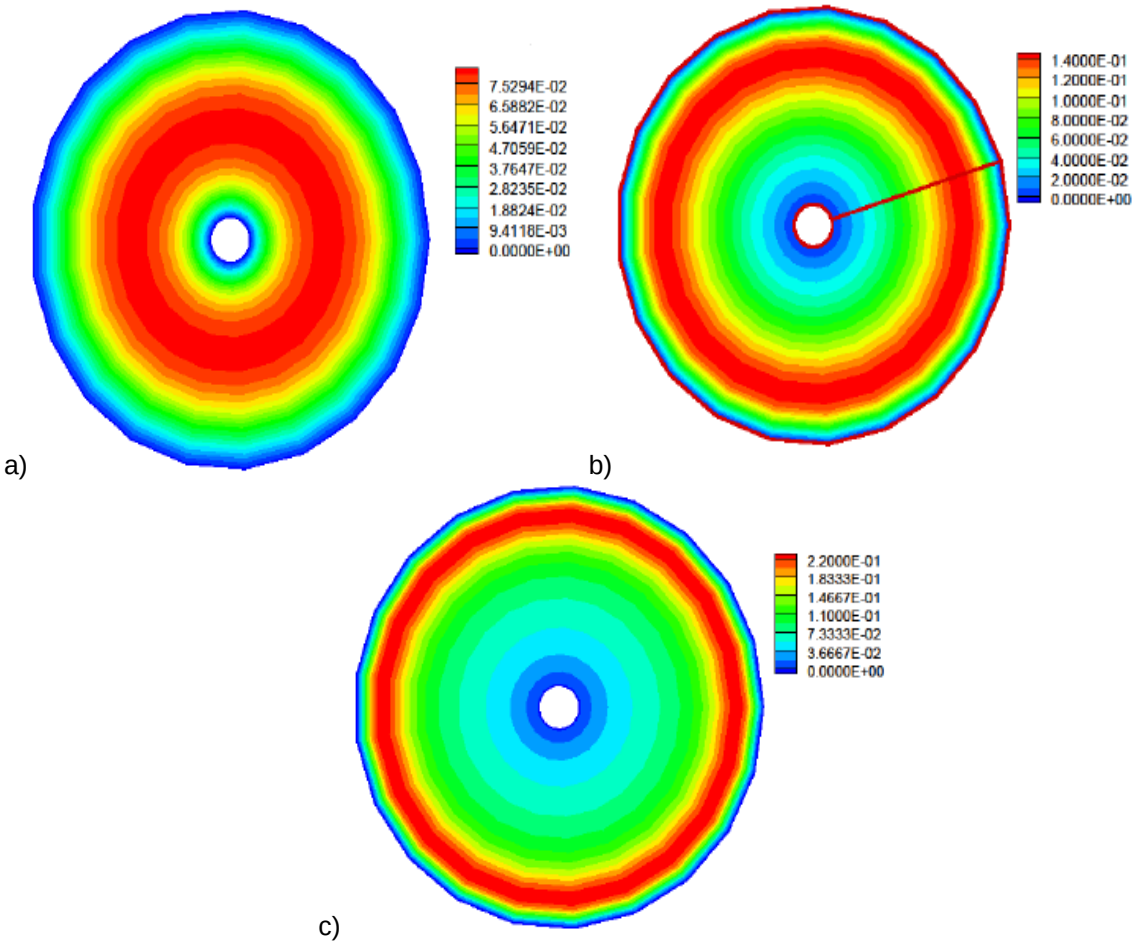

Figure 4. Contours of Azimuthal velocity at different y constant (height) $r-\theta$ plane at Re=1290, AR =1.5, (a) y=0.15, (b) y =0.75 and(c) y =1.35.

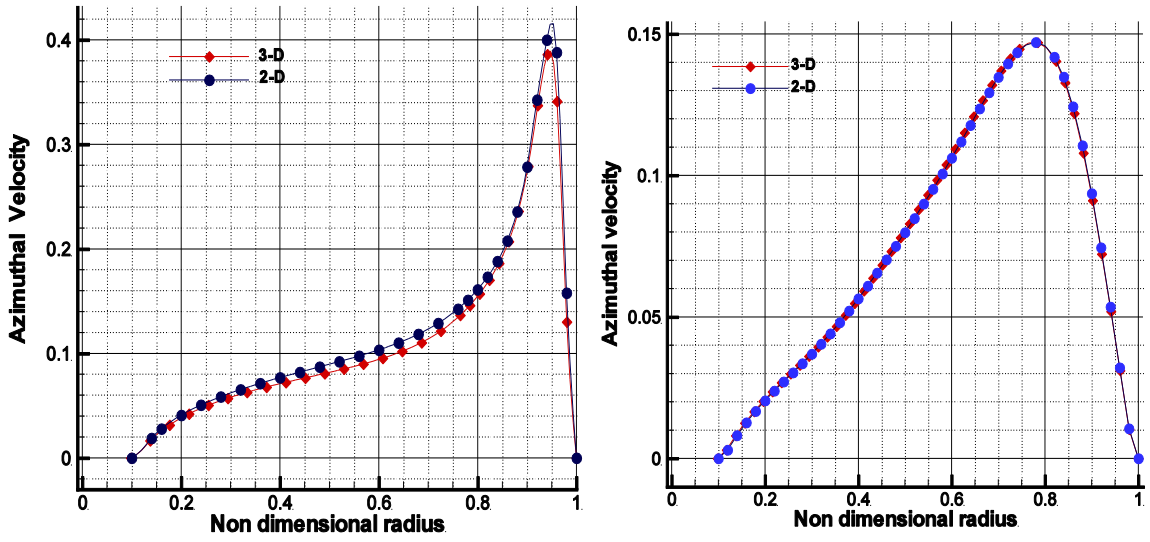

a) y =1.4, b) y=0.75.

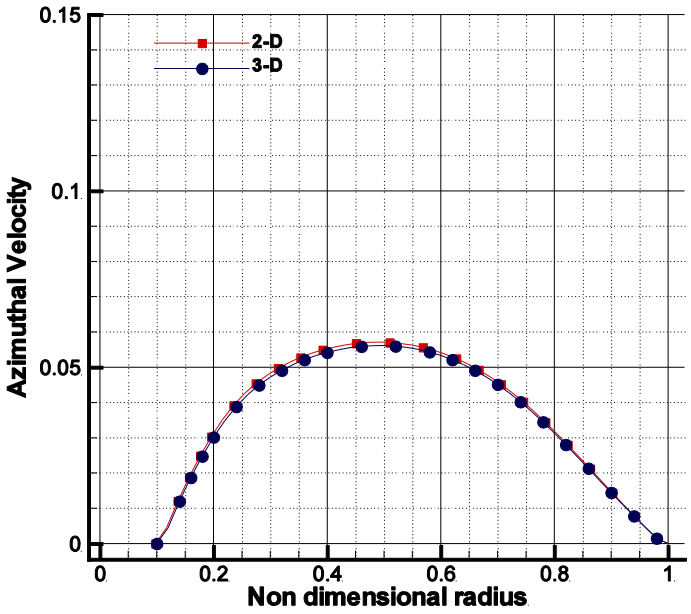

c) y =0.1

Figure 5. Comparisons of Radial profile of azimuthal (angular) velocity component of 2-D with 3-D for Re=1290, AR =1.5 at different axial height along vertical direction (a) y =1.4, (b) y=0.75 (c) y =0.1.

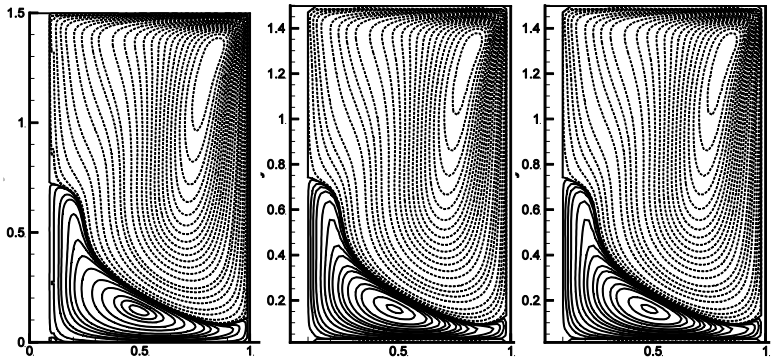

a) 2-D b) $\theta = 80$ c) $\theta = 160$

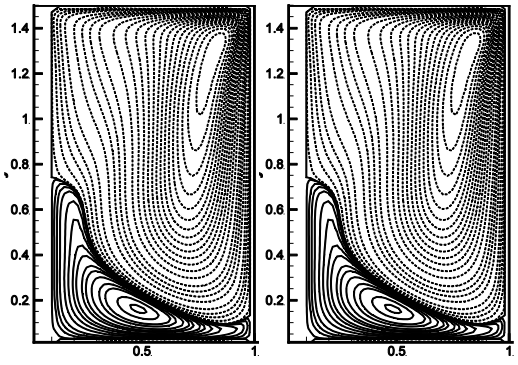

d) $\theta = 240$ e) $\theta = 320$

Figure 6. Contours steam contours in (r-y) meridional plane of cylindrical cavity at Re=1290, AR=1.5, Ri =0.05, Pr=1.0 at different θ When Top Lid at T_h , Bottom Fixed wall at T_C and side vertical walls are insulated.

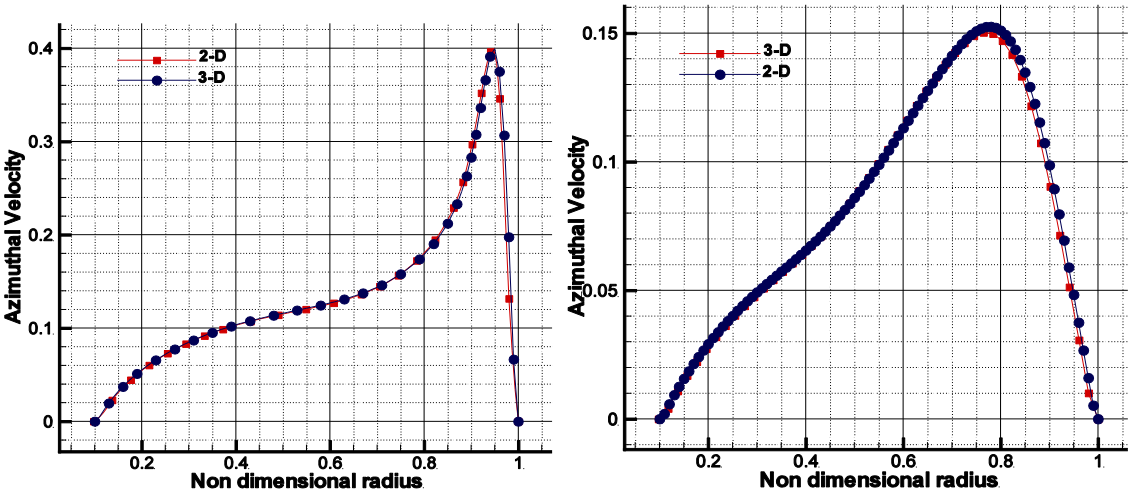

a) y =1.4 b) y=0.75

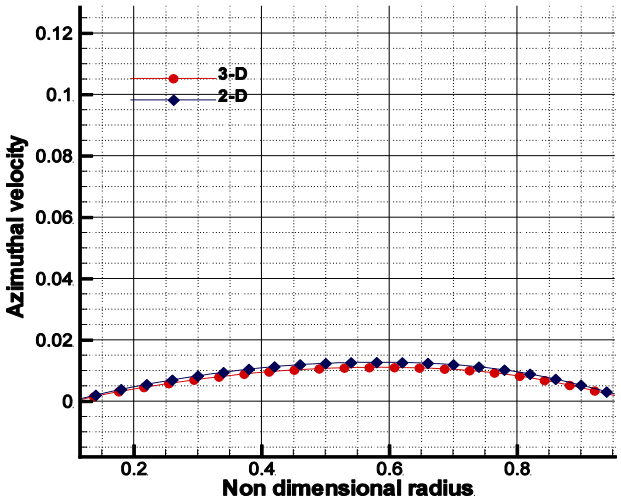

c) y =0.1

Figure 7. Comparison of Radial profile of azimuthal velocity component of 2-D with 3-D for Re =1290, AR =1.5, Pr =1.0, Ri =0.05 at different axial height (a) y =1.4,(b) y=0.75 (c) y =0.1.

Comparison of radial profiles of azimuthal velocities show that this three dimensional effects are negligible as seen from Figure 7. One may also observe the effect of axial heat gradient is to reduce the peak value of the azimuthal velocity near the cooler wall i.e.at y = 0.1 constant plane, Figure 5 c) and Figure 7 c), which is true for both 2-D axisymmetric as well as 3-D case. The contours of isotherms in r-y meridional plane are shown in Figure 8. The isotherms plots of 2-D axisymmetric calculations, Figure 8 a), are almost identical as obtained by 3-D calculations in different $\theta =$ constant planes Figure 8 b) to Figure 8 e).

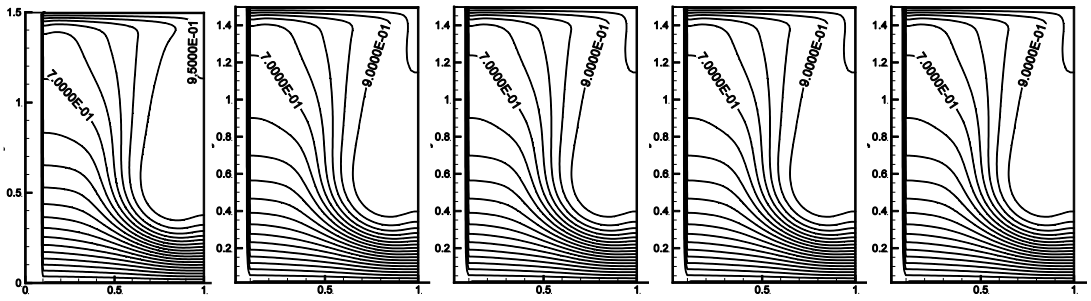

a) 2-D b) $\theta = 80$ c) $\theta = 160$ d) $\theta = 240$ e) $\theta = 320$

Figure 8. Contours of isotherms in (r-y) meridional plane of cylindrical cavity at Re=1290, AR=1.5, Ri=0.05, Pr=1.0 at different θ .

From this study one can conclude that the heat flow also maintains the axisymmetric behavior under the chosen conditions. This axisymmetric behavior can also be observed from the isotherms plotted in $r-\theta$ planes or y=constant planes Figure 9.

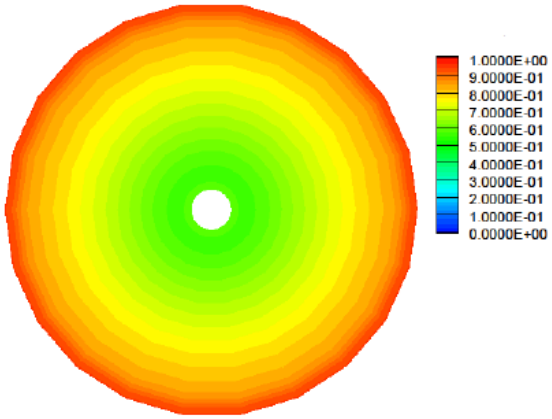

a)

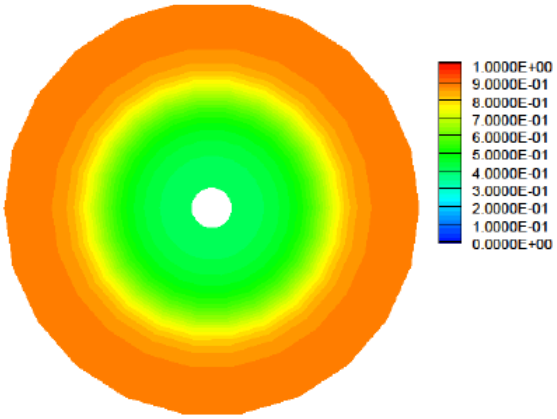

b)

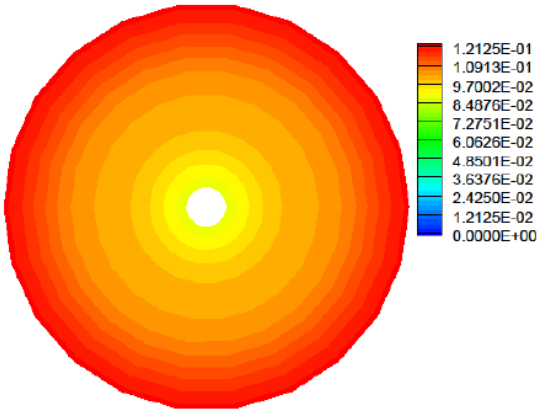

c)

Figure 9. Contours of Isotherms in (r $-\theta$) plane of cylindrical cavity at Re=1290, AR=1.5, Ri =0.05, Pr=1.0 at different height (y-constant plane) (a) y = 0:1(b) y = 0:75, (c) y = 1:4.

To investigate the influence of Re and Ri on the overall heat transfer, the average Nusselt number has been calculated for this annuals cylindrical cavity of Ar=1.5. The average Nusselt number Nu is shown as a function of Re in Figure 10 and as a function of Ri in Figure 11. It can be observed that rate of change Ne with Re decreases drastically as Ri is increased from 0.0 to 1.0. From this one can conclude that the overall heat transfer by convection increases with increase in Re but decreases with increase in Ri.

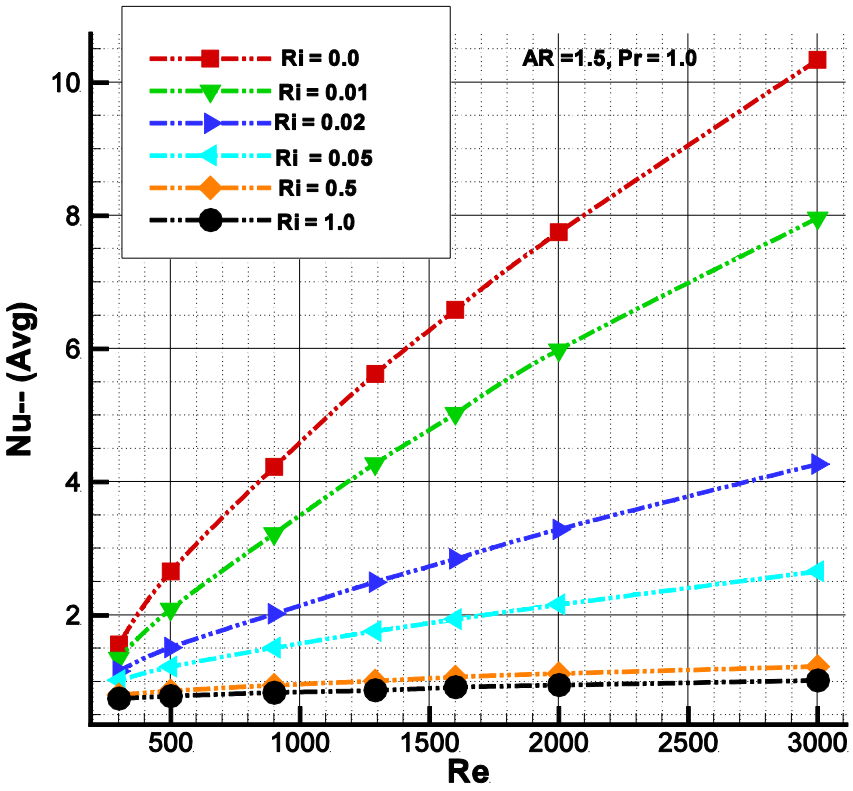

Figure 10. At AR =1.5, Pr= 1.0, for different Richardson number; variation of average Nussent number at different Reynolds number.

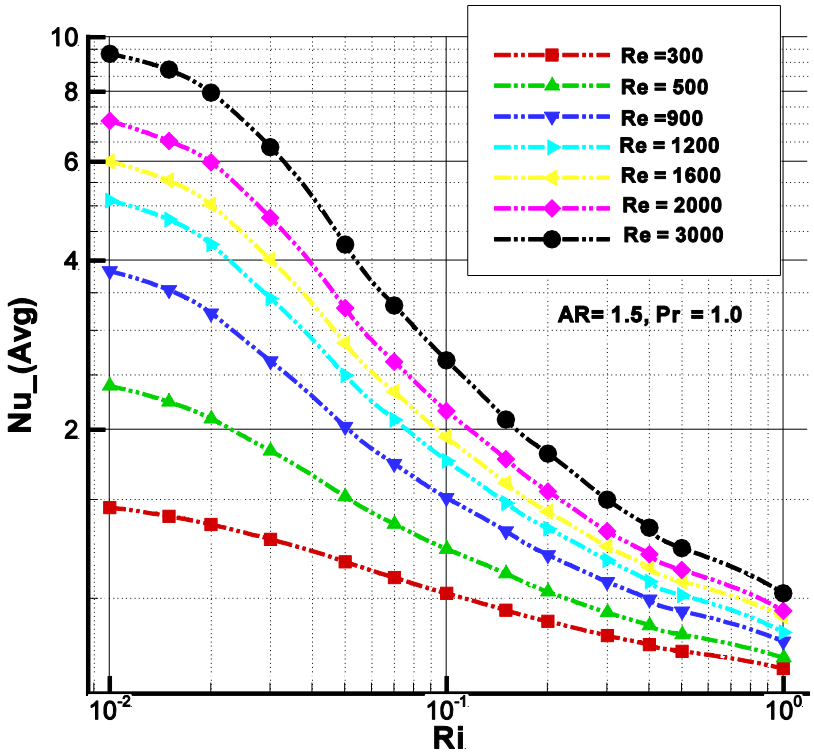

Figure 11. At AR =1.5, Pr= 1.0, for different Reynolds number; variation of average Nussent number at different Richardson number.

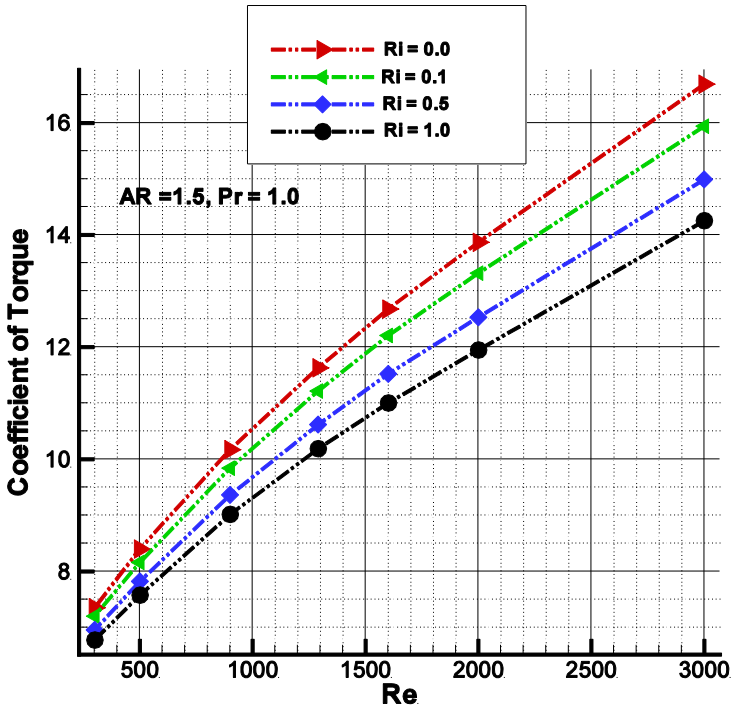

Figure 12. At AR =1.5, Pr= 1.0, for different Richardson number; variation of co-efficient of torque number at different Reynolds number.

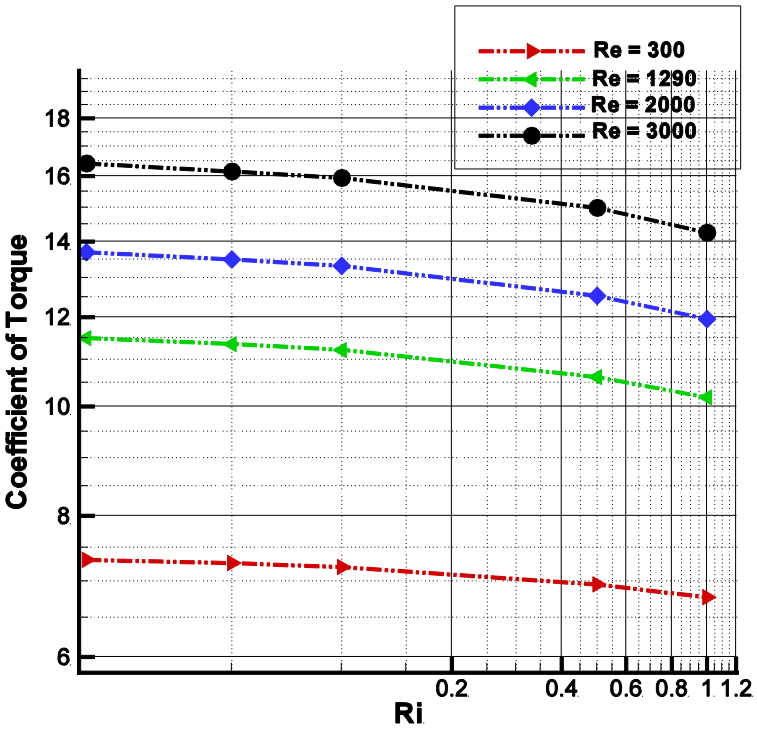

Figure 13. At AR =1.5, Pr= 1.0, for different Reynolds number; variation of coefficient torque at different Richardson number.

For engineering applications one may be interested to calculate torque coefficient C_T necessary to sustain the top disc rotation with uniform speed. Figure 12 shows that C_T is an increasing function of Re.

For a given Reynolds number the value of C_T slightly decreases when Ri is increased over the parameter range covered in the present study as can be seen in Figure 13. Hence, it may be possible to control the magnitude of torque required by appropriately imposing a vertical thermal boundary condition on to end walls of the cavity.

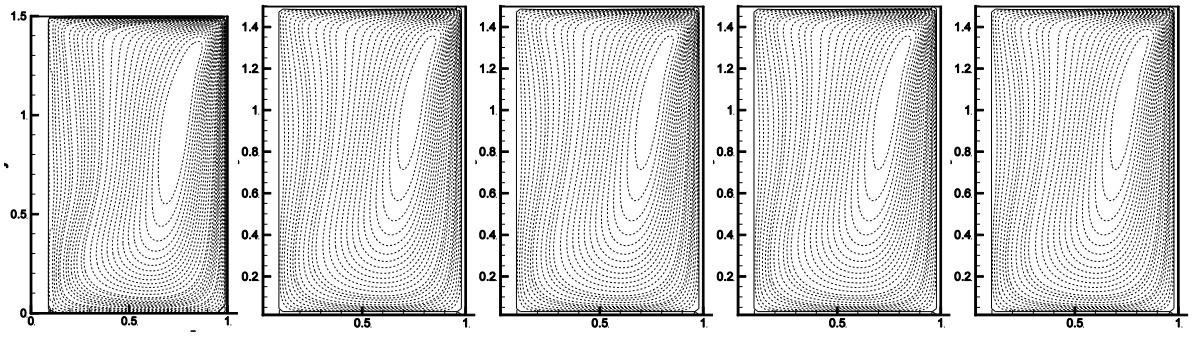

a) 2-D b) $\theta = 80$ c) $\theta = 160$ d) $\theta = 240$ e) $\theta = 320$

Figure 14. Steam contours in different (r-y) meridional plane of cylindrical cavity for Re =1290, AR =1.5, Ha = 10.0.

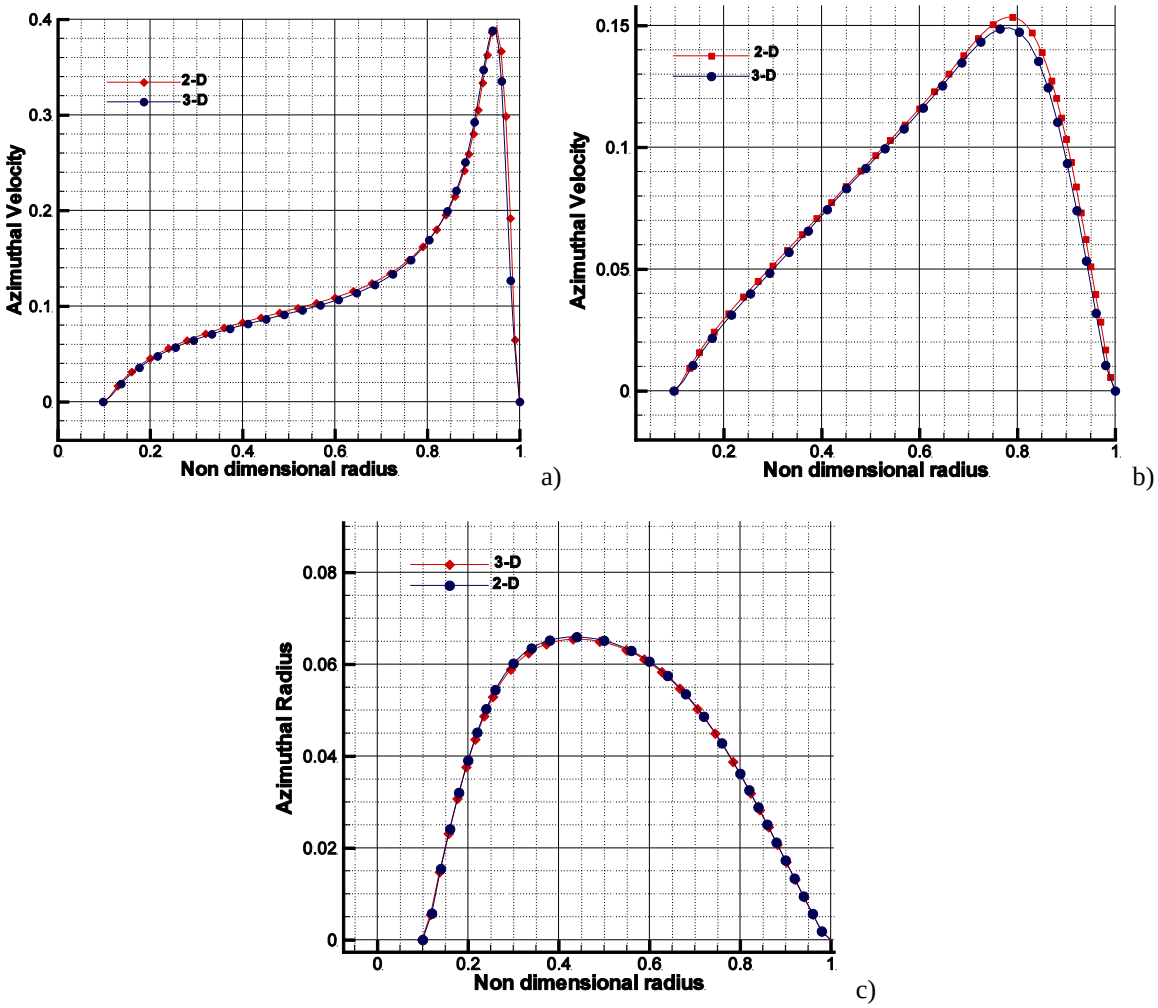

Figure 15. Comparison of Radial profile of azimuthal velocity component of 2-D with 3-D for Re =1290, AR =1.5, Ha = 10.0 at different axial height a) y =1.4, b) y=0.75, c)y =0.1.

Case III (a): 3-D Lid driven swirling flow in a cylindrical annulus with axial magnetic field with Ha=10.0.

Under influence of an axial magnetic field the 3-D swirling flow has been investigated for Re =1290, AR =1.5, and Ha =10. In this case it is assumed that all surfaces of cylindrical annular cavity are electrically insulated. Under these conditions the vortex breakdown completely vanishes as shown in stream contours in r-y plane for both 2-d axisymmetric and 3-d flow situations Figure 14.

Furthermore, from Figure 14 it can be observed that, for the given conditions of the case, the 3-D flow shows axisymmetric behavior under the influence of axial magnetic field. The same can also be observed from the quantitative comparison of the azimuthal velocity in y=constant planes, Figure 15.

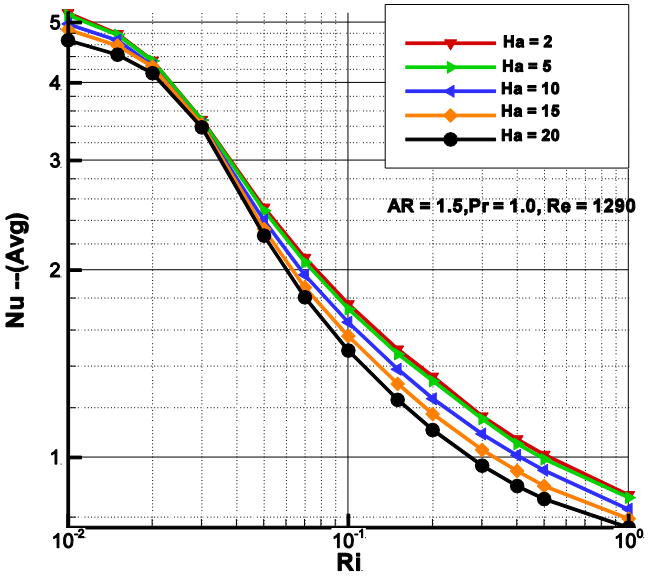

Figure 16. At AR =1.5, Pr=1.0, for different Ha number; variation of average Nusselt number at different Richardson number.

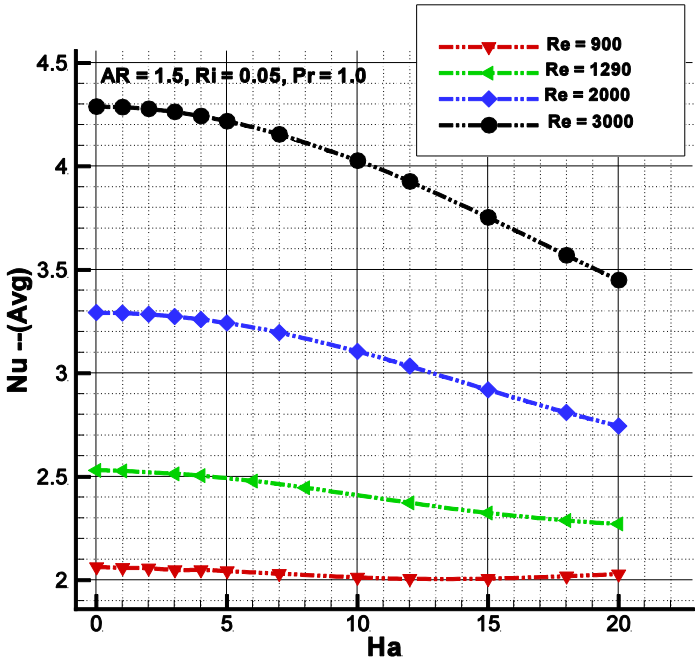

Figure 17. At AR =1.5, Pr=1.0, Ri =0.05, for different Reynolds number number; variation of average Nusselt number at different Ha number.

To analyze the influence axial magnetic field on the heat transfer rate swirling flow in the annuals cavity with both axial heat gradient and axial magnetic field has been studied. Figure 16 shows the variation of Nu with Ri for Hartmann Number Ha ranging from 0 to 20 with fixed values of Pr=1.0 & Re=1290. A slight decrease in the average Nusselt number with increasing value of Ha indicates that the heat transfer by convection decreases with increase of strength of magnetic field. This indicates that the presence of magnetic field tends to suppress the convective heat transfer and its effect increases with increase in Ri. Further, the variation of Nu with Ha for fixed values of Ri=0.05 & Pr=1.0 with Re =900 to 3000 is shown in Figure 17. Form Figure 17 it can be observed that rate of decrease of Nu with Ha reduces slightly with decreasing value of Re.

CONCLUSION

Various simulations of three dimensional lid driven swirling flows, in an annular cavity, with and without axial magnetic field or the axial temperature gradient has also been carried out. It has been observed that within the steady flow zones, with or without vortex breakdowns, the axisymmetric nature of the flow is maintained. Moreover, the effects of governing parameters Re, Ri and Ha on the overall heat transfer has been discussed by investigating the nature of variation of the average Nusselt number with these parameters.

Non-dimensional numbers

$Nu_h = \left.\frac{\partial T}{\partial y}\right|_{y=h}$ Local Nusselt number

$\overline{Nu} = \frac{1}{\pi}\int_0^1 Nu_h(r)2\pi dr$ Average Nusselt number

$C_T = \frac{1}{\pi}\int \left.\frac{\partial u_\theta}{\partial y}\right|_{y=h} 2\pi r^2 dr$ Co-efficient of torque

$Ha = BR\sqrt{\frac{\sigma}{\mu}}, [\sigma]$ Hartmann Number

$N = \frac{Ha^2}{\mathrm{Re}}$ Interaction parameter

Re Reynolds number $\frac{\Omega R^2}{\nu}$

Ri Richardson Number $\frac{g\beta(T_h - T_C)}{R\Omega^2}$

Pr Prandtl Number $\frac{\nu}{\alpha}$

Symbols

AR Aspect ratio = H/R
B Magnetic Field [kg/s^{3}A]
Fl_r. Lorentz force in radial direction [N]
Fl_y Lorentz force in axial direction [N]
Fl_θ Lorentz force in azimuthal direction [N]
g- acceleration due to gravity [m/sec^2]
H Height of cylinder [m]
R Radius of the cylinder[m]
r, h Non-dimensional radius and height of cylinder
p Non-dimensional pressure
r Non-dimensional radius of rotating lid, cylindrical cavity and bottom stationary wall.
r, y Non-dimensional meridional coordinate

T Non-dimensionless Temperature

T_h Non-dimensional temperature at top lid

T_C Non-dimensional temperature at bottom wall

t Non-dimensional time .

u_r, u_θ, u_y Non-dimensional velocity components in the radial azimuthally and axial directions respectively.

Greek Symbol

ν Kinematic viscosity [m^2/sec]

α Thermal diffusivity.[m^2/s]

β Thermal expansion coefficient of fluid.[1/K]

σ Fluid Electrical conductivity[s^3A^2/m^3kg]

μ Dynamic viscosity [kg/m sec]

Ω Constant angular speed of top rotating disc[rad /sec]

ψ Non-dimensional stream function

Δt Discrete time interval

Δx length of each grid element

Δy height of each grid element

$\Delta\theta$ Angular width of each grid element (radian)

Subscripts:

c Cold

h Hot

r, θ, y Radial, Axial and Azimuthal directions, respectively

Φ Electric potential

i, j, k Indices to identify a cell

REFERENCES

[1] Escudier, M. P. "Observations of the flow produced in a cylindrical container by a rotating endwall." *Experiments in fluids* 2, no. 4 (1984): 189-196.

[2] Hourigan, K., L. J. W. Graham, and M. C. Thompson. "Spiral streaklines in pre-vortex breakdown regions of axisymmetric swirling flows." *Physics of Fluids (1994-present)* 7, no. 12 (1995): 3126-3128.

[3] Stevens, José L., Z. Z. Celik, B. J. Cantwell, and J. M. Lopez. "Experimental study of vortex breakdown in a cylindrical, swirling flow." (1996).

[4] Fujimura, Kazuyuki, Hide S. Koyama, and Jae Min Hyun. "Time-dependent vortex breakdown in a cylinder with a rotating lid." *Journal of fluids engineering* 119, no. 2 (1997): 450-453.

[5] Spohn, A., M. Mory, and E. J. Hopfinger."Experiments on vortex breakdown in a confined flow generated by a rotating disc." *Journal of Fluid Mechanics*370 (1998): 73-99.

[6] Blackburn, Hugh M., and J. M. Lopez. "Symmetry breaking of the flow in a cylinder driven by a rotating end wall." *Physics of Fluids* 12, no. 11 (2000): 2698-2701.

[7] Sotiropoulos, Fotis, and Yiannis Ventikos. "The three-dimensional structure of confined swirling flows with vortex breakdown." *Journal of Fluid Mechanics* 426 (2001): 155-175.

[8] Vogel, H. U. 1968: Experimentelle Ergebnisse t~ber die laminare Str6mung in einem zylindrischen Geh~iuse mit darin rotierender Scheibe. MPI Bericht 6.

[9] Ronnenberg, B. 1977: Ein selbstjustierendes 3-Komponenten-Laserdoppleranemometer nach dem Vergleichsstrahlverfahren,angewandt far Untersuchungen in einer station~ tren zylinder symmetrischen Drehstr6mung mit einem Rt~ckstromgebiet. MPI Bericht 20.

[10] Escudier, M. P., and J. J. Keller. Vortex breakdown: a two-stage transition.BROWN BOVERI RESEARCH CENTER BADEN (SWITZERLAND), 1983.

[11] Lopez, J. M. (1990). Axisymmetric vortex breakdown Part 1. Confined swirling flow. Journal of Fluid Mechanics, 221, 533-552.

[12] Lugt, H.J. and Abboud, M., 1987, "Axisymmetric vortex breakdown with and without temperature effects in a container with a rotating lid," Journal of Fluid Mechanics., 179, pp.179-200.

[13] Bessaïh R, Marty P, Kadja M. Numerical study of disk driven rotating MHD flowof a liquid metal in a cylindrical enclosure. Acta Mech 1999; 135:153.

[14] Bessaïh R, Kadja M, Eckert K, Marty P. Numerical and analytical study of rotating flow in an enclosed cylinder under an axial magnetic field. Acta Mech2003; 164:175.
[15] Gelfgat YM, Gelfgat AY. Experimental and numerical study of rotating magnetic field driven flow in cylindrical enclosures with different aspect ratios. Magnetohydrodynamics.2004; 40:147.
[16] Lee, C. H., & Hyun, J. M. (1999). Flow of a stratified fluid in a cylinder with a rotating lid. *International journal of heat and fluid flow*, *20*(1), 26-33.
[17] Kim, W. N., & Hyun, J. M. (1997). Convective heat transfer in a cylinder with a rotating lid under stable stratification. *International Journal of Heat and Fluid Flow*, *18*(4), 384-388.
[18] Iwatsu, R. (2004). Flow pattern and heat transfer of swirling flows in cylindrical container with rotating top and stable temperature gradient. *International journal of heat and mass transfer*, *47*(12), 2755-2767.
[19] Chen, S. (2011). Entropy generation inside disk driven rotating convectional flow. *International Journal of Thermal Sciences*, *50*(4), 626-638.
[20] Dash S., and Singh N., 2016, **"**Effects of Partial Heating of Top Rotating Lid With Axial Temperature Gradient On Vortex Breakdown In Case Of Axisymmetric Stratified Lid Driven Swirling Flow," Yildiz Technical University Press, Istanbul, Turkey , J. Thermal Eng., 2(Sp. Issue 4), pp. 883-896.
[21] Gefagat A. Y. , Destabilization of free convection by weak rotation, 9th international conference heat transfer fluid mechanics and thermodynamics,16-18 july 2012,Malta.
[22] Bessaïh R, Boukhari A, Marty P. Magnetohydrodynamics stability of a rotatingflow with heat transfer. Int Commun Heat Mass 2009; 36:893.
[23] Mahfoud B, Bessaih R. Oscillatory swirling flows in a cylindrical enclosure with co-/counter-rotating end disks submitted to a vertical temperature gradient. Fluid Dynamics & Materials Processing. 2012; 8:1.
[24] Verzicco, R., and P. Orlandi. "A finitedifference scheme for three-dimensional incompressible flows in cylindrical coordinates." *Journal of Computational Physics* 123, no. 2 (1996): 402-414.
[25] Barbosa, Emerson, and Olivier Daube. "A finite difference method for 3D incompressible flows in cylindrical coordinates." *Computers & fluids* 34, no. 8 (2005): 950-971.
[26] Fukagata, Koji, and Nobuhide Kasagi. "Highly energy-conservative finite difference method for the cylindrical coordinate system." *Journal of Computational Physics* 181, no. 2 (2002): 478-498.
[27] Chorin, A. J., A Numerical method for solving incompressible viscous flow problems, Journal of Comput. Phys., Vol 2, pp 12-26, 1967.
[28] Peyret, R.&Taylor, D.(1983*)*. Computational methods for fluid flow;SprigerVerlag.